Asian Journal of Chemistry; Vol. 38, No. 2 (2026), 463-470
ASIAN JOURNAL OF CHEMISTRY
https://doi.org/10.14233/ajchem.2026.35201

Study on Adsorption Efficiency of Low-Cost Hemp Seed Oil Cake (*Cannabis sativa* L.) as Adsorbent for the Removal of Reactive Black 5 Dye from Aqueous Solution

ADELLA MYORI HARDIEKA and TÜRKAN BÖRKLÜ BUDAK*

Department of Chemistry, Faculty of Art and Science, Yildiz Technical University, 34220 İstanbul, Türkiye

*Corresponding author: E-mail: tborklu@yildiz.edu.tr; turkanborklu@yahoo.com

Received: 6 November 2025 *Accepted*: 10 January 2026 *Published online*: 31 January 2026 AJC-22264

Driven by the need for sustainable and economical water treatment solutions, this study explores the use of agricultural byproduct adsorbents, specifically hemp seed oil cake (HSOC), for the removal of reactive black 5 (RB5) dye. Batch experiments identified the ideal conditions for the adsorption process, resulting in a maximum removal efficiency of 99.94%. The process, identified as spontaneous and exothermic through thermodynamic analysis, was most effective under the following conditions: an initial RB5 dye concentration of 10 mg/L, 1.5 g of HSOC adsorbent, a pH of 4 (acidic condition), 45 min of contact time, 100 rpm agitation and a temperature of 50 ºC. These results collectively affirm HSOC's promise as a highly efficient, bio-based material for the remediation of dye-contaminated water.

Keywords: Adsorption, Hemp seed oil cake, Reactive black 5, Textile effluent, Water treatment.

INTRODUCTION

The advancement of industry and technology has led to widespread dependency on synthetic dyes across multiple sectors, including textiles, plastics, paper, rubber, leather and pharmaceuticals for product colouration. This dependency is concerning given the recalcitrant nature of these compounds, which poses a significant environmental threat due to their resistance to microbial degradation [1]. The textile industry is the most detrimental in terms of effluent volume and composition, presenting significant difficulties for traditional biological wastewater treatment processes [2-4]. The synthetic dye market is substantial, with an annual global output estimated at 7×10^5 tons of dyestuff, encompassing a diverse array of chemical classes such as azo, reactive, anthraquinone and metal-complex dyes [5,6].

Despite its widespread application in the textile industry owing to its cost-effectiveness and durability, the anionic diazo dye reactive black 5 (RB5) is resistant to biodegradetion. Its discharge in textile effluent leads to significant water discolouration, which diminishes light penetration and disturbs aquatic ecosystems. An additional hazard is the potential release of carcinogenic aromatic amines during its degradation [7]. Consequently, the elimination of dyes from wastewater is a critical objective, driving significant interest in the development of remediation technologies for dye-contaminated water.

Nowadays, a variety of physical, chemical and biological techniques are available for toxic dye removal, including membrane filtration [8], advanced oxidation process [9,10], ion exchange [11], coagulation-flocculation [12,13], adsorption [14], electrochemical [15,16], chemical precipitation [17], photocatalytic degradation [18] and ozonation [19,20]. Due to its operational simplicity, cost-effectiveness, high efficiency and the potential for recyclability, adsorption is widely recognised as the preferred technique for treating industrial dye effluents [21-23]. The effectiveness of adsorption is directly determined by the adsorbent's characteristics.

Agricultural waste offers a sustainable, low-cost solution for removing toxic dyes and heavy metals from industrial wastewater, serving as a viable alternative to expensive commercial activated carbon [24]. The primary advantage is cost-effectiveness, as these organic materials are readily available as byproducts, significantly reducing production costs [25]. A wide variety of agricultural wastes have been extensively researched and proven effective for this purpose. These include biodegradable materials such as longan peel [26], potato peel [27], jackfruit peel [28], rice husk [29], peanut husk [30], coffee grounds [31,32], silybum marianum stem [33], mul-

berry leaves [34,35], linden leaves [36], walnut shell [37], chestnut shell [38], apricot kernel shell [39], corn stalk [40], sawdust [41] and others.

Originating in China, the ancient crop hemp (*Cannabis sativa* L.) spread across Asia, the Middle East and Europe *via* established trade routes. The solid byproduct of hemp seed oil extraction, hemp seed oil cake (HSOC), is valued not only for its nutritional applications in animal feed and human food but also for its promise as a sustainable adsorbent for wastewater treatment [42]. A key advantage of HSOC over other agricultural waste adsorbents is due to its protein-rich composition. This composition yields a high concentration of amine and carboxyl functional groups, which serve as potent active sites for chemisorption. As a result, HSOC frequently exhibits superior adsorption capacities for contaminants such as heavy metals [43] and dyes [44], often with minimal pretreatment needed. This inherent functional diversity enables HSOC to achieve high removal efficiency across a broader spectrum of pollutants compared to adsorbents derived from predominantly lignocellulosic waste materials [45].

The primary objective of this study was to evaluate the potential of HSOC as an economical and eco-friendly adsorbent for removing RB5 azo dye from aqueous solutions. A batch adsorption method was used to investigate the effects of critical parameters *viz*. initial pH, adsorbent dosage, initial dye concentration and contact time. These variables were quantified to determine the optimal conditions for achieving the highest possible dye removal and adsorption capacity.

EXPERIMENTAL

Hemp seed oil cake (HSOC) as a sustainable adsorbent was obtained from Cansızzade Bitkisel Yağlar herbalist in İstanbul, Türkiye. Reactive black 5 dye (m.w. = 991.82 g/mol; m.f. = $C_{26}H_{21}N_5Na_4O_{19}S_6$; λ_{max} = 597 nm) as an adsorbate in the adsorption studies was supplied from Sigma-Aldrich. The effect of initial pH on the adsorption process was studied using buffer solutions at pH 4 (citrate), 7 (phosphate) and 10 (carbonate). The HSOC adsorbent used in this study is depicted in Fig. 1.

Fig. 1. Hemp seed oil cake (HSOC) for the adsorption of RB5 dye

General procedure: A 1000 mg/L stock solution of RB5 dye was prepared by dissolving an accurately measured amount in distilled water from a purification system (Mikrotest MSD-08). Subsequent experimental solutions were prepared by diluting this stock with an appropriate amount of distilled water. The adsorption process was carried out in a shaking water bath that controlled temperature (Julabo SW22). The pH of the solution was monitored with a pH meter (WTW InoLab Cond pH 720). The amount of adsorbed dye was then determined by analyzing its concentration using a UV-Vis spectrophotometer (Agilent 8453) at the RB5 dye's maximum wavelength (λ_{max}) of 597 nm. To determine the functional groups in the HSOC structure responsible for RB5 dye adsorption, measurements were performed using a Nicolet IS10 FTIR spectrometer (FTIR-ATR; Nicolet IS10). Similarly, scanning electron microscopy (SEM; Zeiss EVO LS10) was used to elucidate the morphological changes occurring during adsorption.

Adsorption process: Batch experiments were conducted to study the adsorption of RB5 dye onto HSOC adsorbent. The experimental conditions systematically assessed the influence of several parameters, including adsorbent dose (0.1-1.5 g), initial pH (4-10), initial RB5 dye concentration (10-50 mg/L), temperature (25-50 ºC), stirring speed (100-180 rpm) and contact time (5-180 min). In each test, 50 mL of RB5 dye solution was agitated with a specified amount of HSOC adsorbent in a temperature-controlled water bath shaker. After the set time, the mixture was filtered and the remaining dye concentration in the filtrate was determined by measuring its absorbance with a UV-Vis spectrophotometer. The initial and final absorbance measurements were then used in eqns. 1 and 2 to determine the percentage removal (%R) and the equilibrium adsorption capacity (Q_e) of the dye onto the HSOC adsorbent, respectively.

$$R\ (\%) = \frac{C_o - C_e}{C_o} \times 100 \quad (1)$$

$$Q_e = \frac{C_o - C_e}{m} \times V \quad (2)$$

Where C_o and C_e represent the initial and equilibrium concentrations (mg L^{-1}) of the RB5 dye; V denotes the solution volume (L); m indicates the mass (g) of HSOC adsorbent.

RESULTS AND DISCUSSION

Adsorbent characterisation

SEM studies: The SEM image of HSOC before adsorption revealed an irregular and rough surface morphology (Fig. 2), while significant particle accumulation and surface coating were observed after RB5 adsorption. The morphological changes after adsorption indicate that the dye molecules occupy the active surface regions and that the adsorption process induces physical changes on the surface.

Studies of pH zero-point charge: The critical pH for HSOC was determined to be 5.4, as shown in Fig. 3. Below this value, the adsorbent surface became protonated and acquired a positive charge. The finding of an optimum pH value of 5.4 in experimental studies can be explained by strong

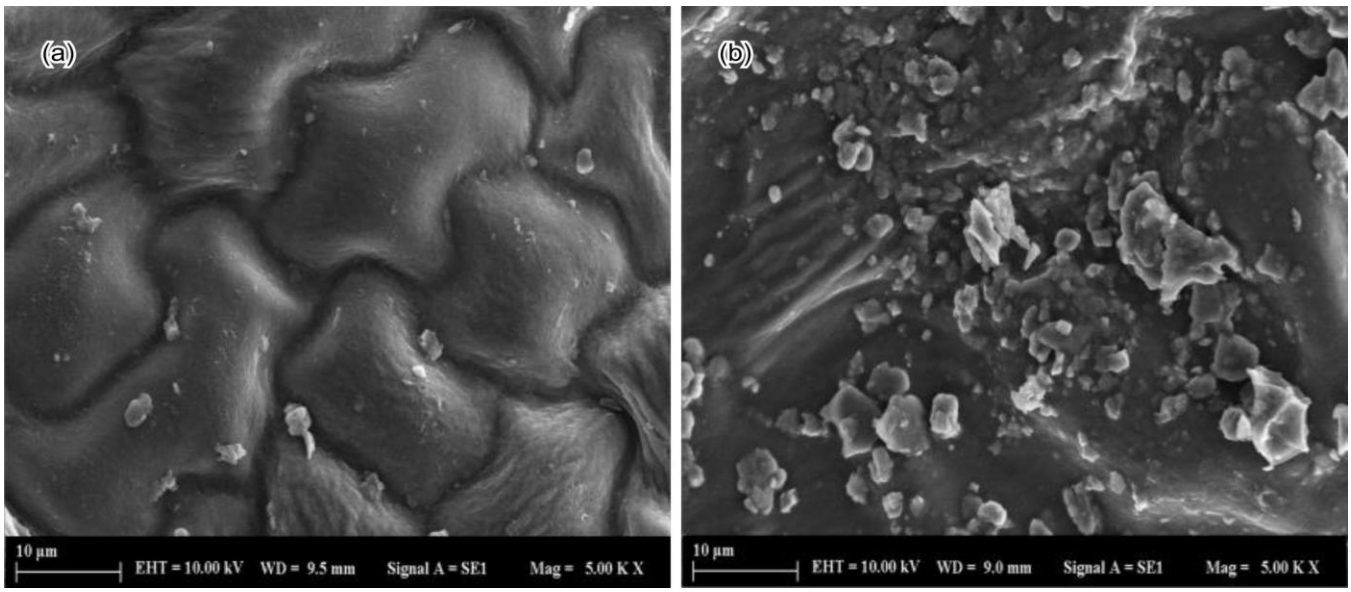

Fig. 2. SEM images of HSOC before (a) and after (b) adsorption

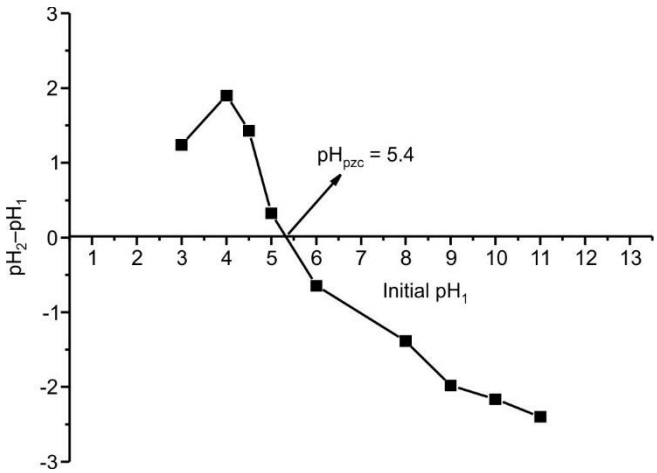

Fig. 3. pH_{pzc} datas of HSOC adsorbent

electrostatic attractions between the anionic RB5 dye molecules and the positively charged adsorbent surface [46]. As the pH rises above the critical pH, the surface charge becomes negative, increasing electrostatic repulsion and decreasing adsorption efficiency.

FT-IR results: As shown in Fig. 4, the intense, broad band at 3277.75 cm^{-1} is attributed to cellulose-derived –OH groups and to the possible formation of hydrogen bonds during adsorption. Similarly, the bands at 2922.83 and 2852.24 cm^{-1} support surface interactions of aliphatic groups during RB5 adsorption *via* C–H stretching vibrations. The band at 1743.17 cm^{-1}, described as the carbonyl (C=O) band, is interpreted as an ester carbonyl stretch originating from cellulose or fatty acid structures. The band around 1632.65 cm^{-1} is associated with aromatic C=C vibrations that explain the lignin structure in the biomass. Similarly, the band at 1515.53 cm^{-1}, representing lignin-

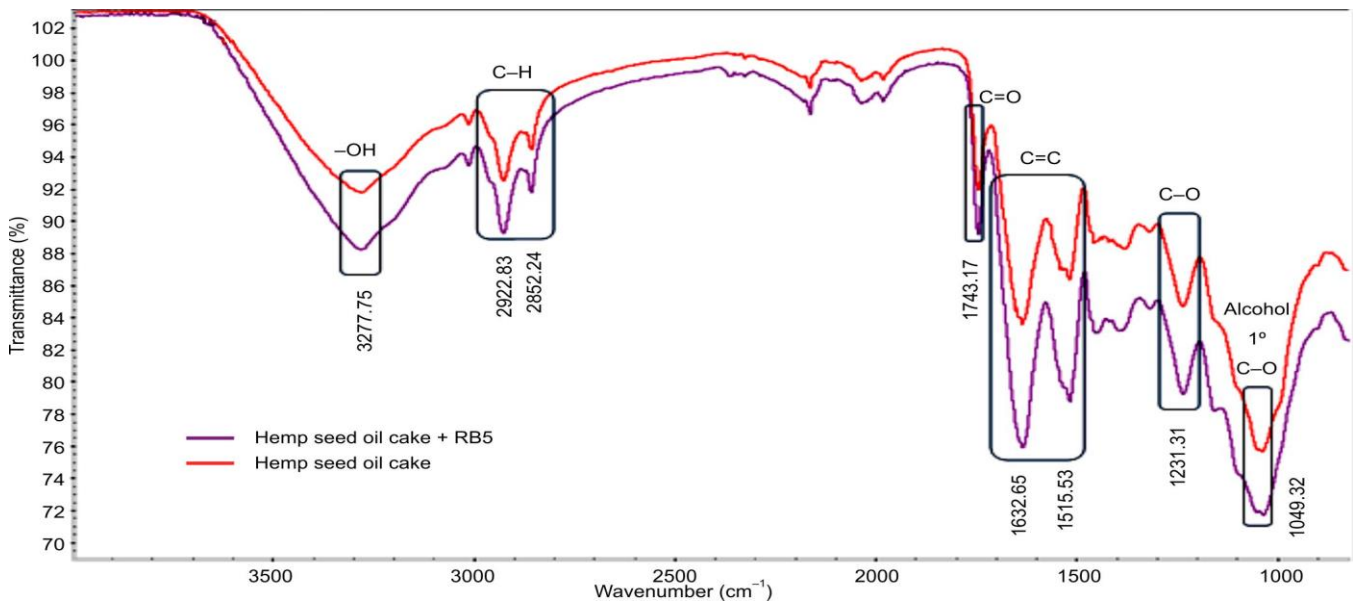

Fig. 4. FT-IR spectra of HSOC powder before and after adsorption of RB5

specific aromatic skeleton vibrations (C=C), confirms the presence of lignin in the sample. Bands at lower wavelengths, such as 1231.31 cm^{-1}, can be associated with C–O stretching vibrations of aryl-alkyl ether bonds in the lignin structure, while the 1049.32 cm^{-1} band can be associated with cellulose derived C–O and C–O–C vibrations (polysaccharide structures). As the obtained FT-IR findings show, the presence of hydroxyl (–OH), carbonyl/ester (C=O), ether (C–O–C) and aromatic functional groups on the HSOC surface suggests that the RB5 anionic dye can be adsorbed *via* hydrogen bonding, dipole-dipole interactions and aromatic π-π interactions [2].

UV-visible studies: To determine the maximum absorbance wavelength of reactive black 5 (RB5) dye, peaks observed between 350-750 nm in the UV-Vis spectrum were examined. The absorption spectrum shown in Fig. 5 exhibited a maximum absorbance in the 597-600 nm range; therefore, a wavelength of λ_{max} = 597 nm was selected for all subsequent analyses. The standard calibration curve for RB5 is presented in Fig. 6. The linear relationship between absorbance (A) and concentration (C) was described by the equation A = 0.0798C – 0.009, with a correlation coefficient (R^2) of 0.9996, indicating excellent linearity and confirming compliance with the Beer-Lambert law over the studied concentration range.

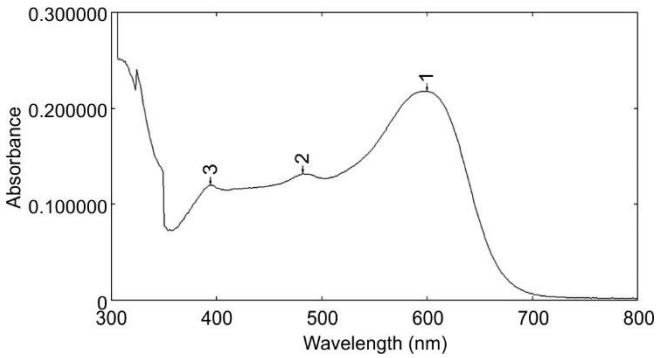

Fig. 5. The determination of the λ_{max} value of the RB5 dye

Adsorption experiments: The results of the studies conducted to determine the optimum operating parameters for the adsorption experiments using HSOC as the adsorbent are presented below.

Effect of adsorbent dosage: To investigate the influence of adsorbent dosage, varying amounts of HSOC (0.1-1.5 g) were added to 50 mL of a 30 mg/L RB5 dye solution. The samples were agitated at 180 rpm and a controlled temperature of 25 ± 0.2 ºC for 30 min. The dye concentration remaining in the filtered solutions was quantified by measuring the absorbance at 597 nm. The resulting effects on both removal efficiency (%R) and equilibrium adsorption capacity (Q_e) are shown in Fig. 7.

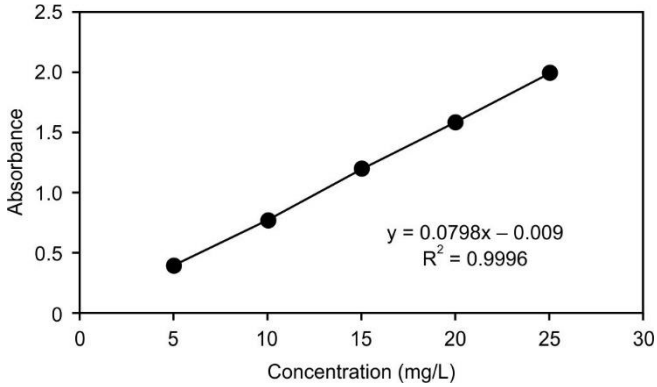

Fig. 6. The standard measurement curve for the RB5 dye

The removal efficiency improved substantially, rising from 22.25% to 94.21% as the adsorbent dosage increased from 0.1 to 1.5 g. This positive correlation reflects the proportional expansion of the total surface area and a concomitant increase in the number of available adsorption sites. In contrast, the equilibrium adsorption capacity decreased markedly, declining from 1.11 to 0.31 mg/g over the same dosage range. The inverse relationship can primarily be attributed to the reduction in the concentration gradient between the solution and the adsorbent. At higher adsorbent dosages, a fixed amount of dye is distributed over a larger number of available adsorption sites, resulting in a lower dye uptake per unit mass of adsorbent and, consequently, a decrease in the equilibrium adsorption capacity.

Effect of initial RB5 dye concentration: To investigate the influence of initial RB5 dye concentration on its adsorption onto the HSOC adsorbent, the experiments were conducted across a concentration range of 10 to 50 mg/L. The experiments were conducted under constant parameters at 25 ± 0.2 ºC and 180 rpm for 30 min. The optimal equilibrium performance, in terms of both removal efficiency and adsorption capacity, was achieved at the lowest initial concentration of 10 mg/L, as shown in Fig. 8.

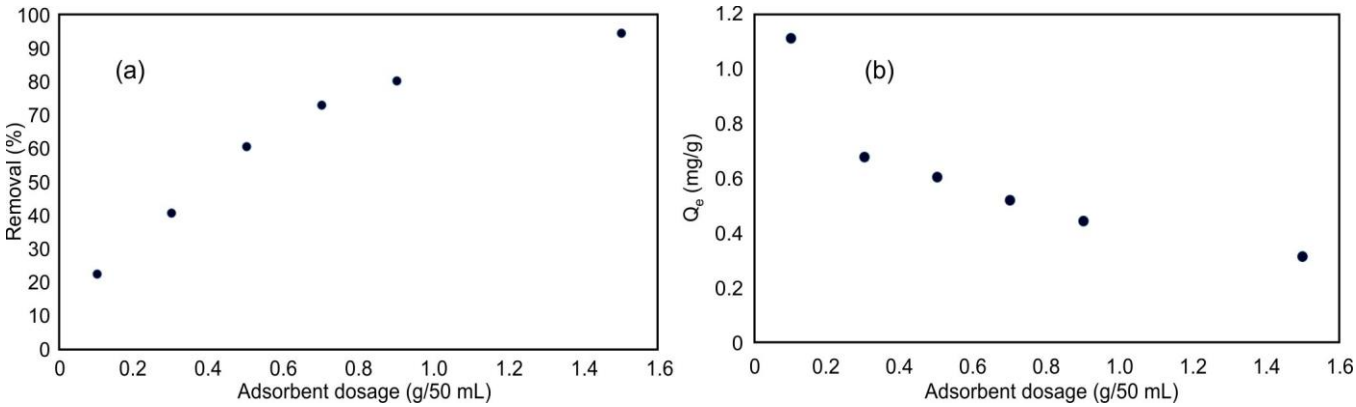

Fig. 7. Influence of HSOC adsorbent dosage on the (a) adsorption efficiency (%R) and (b) adsorption capacity (Q_e) of RB5 dye

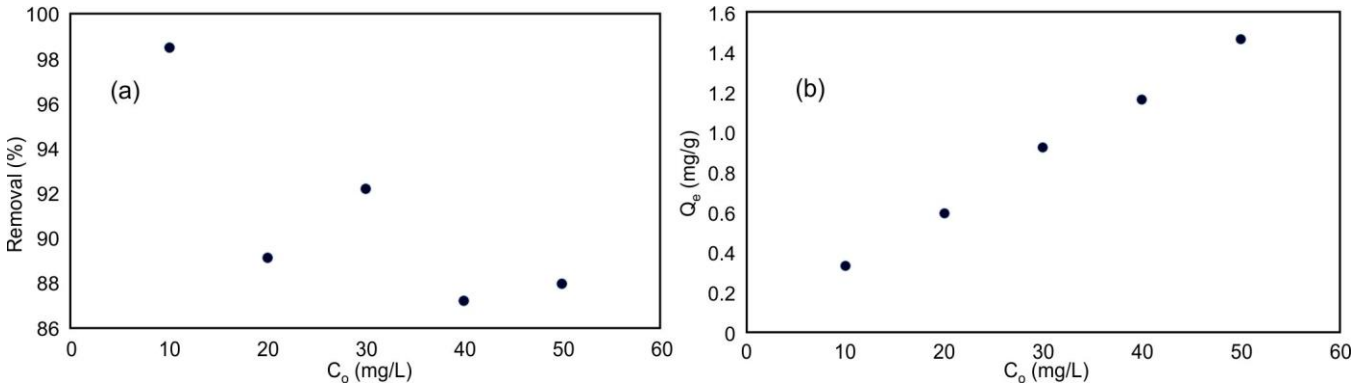

Fig. 8. Influence of initial RB5 dye concentration on RB5 dye (a) removal efficiency (%R) and (b) adsorption capacity (Q_e) on HSOC adsorbent

Higher initial dye concentrations reduced adsorption efficiency (%R) while increasing the adsorbent's capacity (Q_e). This apparent divergence can be explained by the saturation dynamics of the adsorbent's active sites. A high number of available surface sites at low dye concentrations results in high removal efficiency. Conversely, at elevated initial concentrations, the increased driving force for mass transfer and the greater availability of dye molecules lead to the uptake of a larger absolute quantity of adsorbate, thereby enhancing the overall adsorption capacity despite a reduction in the relative removal percentage [47].

Effect of contact time: To assess the impact of contact time on RB5 dye adsorption, a series of batch experiments was conducted. Under set conditions (10 mg/L dye, 1.5 g adsorbent, 100 rpm, 50 ± 0.2 ºC), dye removal was measured at intervals from 5 to 180 min. The results, shown in Fig. 9, indicate that the highest removal rate of 99.87% was achieved after 45 min of contact, identifying this as the time needed to reach equilibrium. The removal efficiency of RB5 dye increases with contact time until an optimum is reached. After this peak, a decrease is observed until a dynamic equilibrium is achieved, a phenomenon attributed to the progressive occupancy and eventual saturation of the adsorbent's binding sites. Consequently, the optimum contact time for RB5 dye adsorption was established at 45 min, determined by analyzing this equilibrium state.

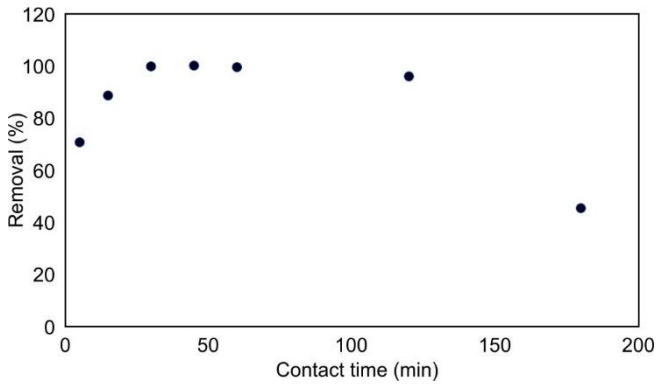

Fig. 9. Influence of contact time on the removal efficiency (%R) of RB5 dye on HSOC adsorbent

Effect of temperature: The influence of temperature on the adsorption efficiency of RB5 was examined over a range of 25 to 50 ºC. Considering the critical influence of temperature on thermodynamic analysis, adsorption experiments were conducted under well-defined and controlled conditions. A constant initial RB5 concentration of 10 mg/L, HSOC dosage of 1.5 g, contact time of 30 min and stirring speed of 180 rpm were maintained to isolate the effect of temperature on the adsorption performance. The adsorption process was found to be endothermic, as evidenced by a positive correlation between temperature and removal efficiency. Fig. 10 shows that increasing the temperature from 25 to 50 ºC increased the RB5 dye removal efficiency (%R) from 80.96% to a maximum of 99.94% at 50 ± 0.2 ºC.

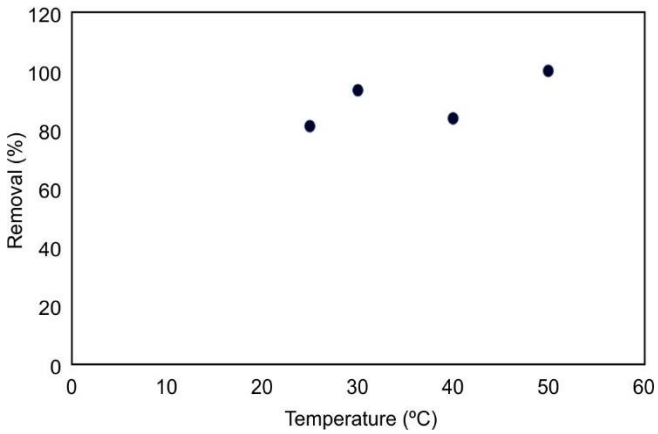

Fig. 10. Influence of temperature on RB5 removal efficiency (%R)

Effect of stirring speed: The impact of stirring speed on RB5 dye adsorption was investigated by testing a range of 100 to 180 rpm. All other parameters, including the amount of HSOC adsorbent (1.5 g), RB5 dye concentration (10 mg/L in 50 mL), contact time (30 min) and temperature (50 ± 0.2 ºC), were held constant to ensure only the agitation intensity varied. After the sample solutions were filtered, the absorbance values were measured at the dye's maximum wavelength of 597 nm. As shown in Fig. 11, a stirring speed of 100 rpm yielded the highest removal efficiency at 99.89%. Excessive mechanical agitation promotes interparticle abrasion within the adsorbent matrix, leading to its fragmentation into fine particles that hinder efficient filtration. Moreover, overly vigorous agitation can compromise the structural integrity of the adsorbent, ultimately diminishing its adsorption performance [48].

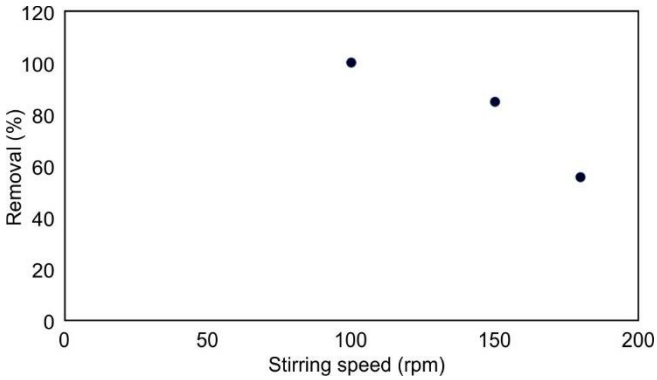

Fig. 11. Influence of stirring speed on the adsorption efficiency (%R) of RB5 dye

Effect of pH: The initial pH of the dye solution plays a crucial role in adsorption efficiency (%R) by affecting the ionisation and surface charge of dye. The impact on RB5 dye removal was tested at pH 4, 7 and 10 using buffer solutions. Under constant conditions, the effect of initial pH on RB5 dye adsorption is shown in Fig. 12. The tests were performed with 10 mg/L of RB5 dye, 1.5 g of HSOC adsorbent in a 50 mL solution, stirred at 100 rpm and held at 50 ± 0.2 ºC for 30 min. The results indicate that the HSOC adsorbent showed high adsorption at low pH values (acidic conditions). This optimum is a result of the surface properties of the HSOC adsorbent interacting with the anionic dye (RB5 dye). At pH 4, the adsorbent surface becomes positively charged, developing a strong electrostatic attraction with the dye anions and leading to high removal rates of 99.94%.

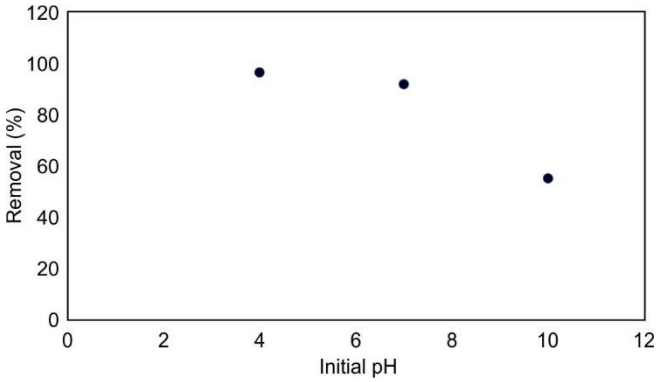

Fig. 12. Influence of initial pH on the RB5 dye adsorption efficiency (%R)

Thermodynamic studies: The thermodynamic parameters for the adsorption of RB5 onto HSOC were evaluated using the apparent distribution coefficient ($K_d = q_e/C_e$) obtained at different temperatures [49]. The standard Gibb's free energy change (ΔG^o) was calculated using the following equation:

$$\Delta G^o = -RT \ln K_d$$

where R is the universal gas constant (8.314 J mol^{-1} K^{-1}) and T is the absolute temperature (K).

The values of enthalpy change (ΔH^o) and entropy change (ΔS^o) were determined from the slope and intercept of the Van't Hoff plot according to:

$$\ln K_d = -\frac{\Delta H^o}{R}\frac{1}{T} + \frac{\Delta S^o}{R}$$

As shown in Table-1, positive ΔG^o values at 25-40 ºC (298-313 K) indicate that adsorption of RB5 onto HSOC does not occur spontaneously at lower temperatures, whereas the negative ΔG^o value at 50 ºC (323 K) confirms that the adsorption process is thermodynamically spontaneous at higher temperatures. The positive enthalpy change (ΔH^o) shows that adsorption of RB5 onto HSOC is endothermic and that higher temperatures support dye uptake, which shows that the maximum adsorption value occurs at 50 ºC. Furthermore, the positive entropy change (ΔS^o) indicates an increase in randomness at the solid-solution interface, which can be interpreted as a structural rearrangement of surface functional groups during adsorption and partial dissolution of RB5 molecules.

TABLE-1
THERMODYNAMIC PARAMETERS FOR RB5 ADSORPTION ONTO HEMP SEED OIL CAKE

Temperature (K)	Thermodynamic parameters		
	ΔG^o (kJ/mol)	ΔH^o (kJ/mol)	ΔS^o (J/mol K)
298	+10.56	+218.10	+699.95
303	+1.76		
313	+4.63		
323	–10.78		

Comparison of adsorption capacity of RB5 dye with different adsorbents: Some studies on the removal of RB5 dye are shown in Table-2. Based on these data, it can be seen that effective removal values can be achieved for RB5 dye from aqueous media using HSOC, due to its natural and abundant presence.

TABLE-2
THE REMOVAL DATA ABOUT THE RB5 DYE USING DIFFERENT ADSORBENT MATERIALS

Adsorbent	Removal efficiency (%)	Ref.
Longan peel activated carbon	83–90	[49]
Kaolin filter cake activated carbon	>90 %	[50]
Laccase-modified silica füme	~95 %	[51]
CNT adsorbents	98–100 %	[52]
Hemp seed oil cake	99.94 %	Present study

Conclusion

The potential of hemp seed meal (HSOC), an agricultural byproduct, as an economical and environmentally friendly adsorbent for removing reactive black 5 (RB5) dye from aqueous solutions was systematically investigated. The experimental results revealed that the optimum conditions for achieving the highest dye removal efficiency were an initial RB5 dye concentration of 10 mg/L, a mass of 1.5 g of adsorbent, pH 4, a temperature of 50 ± 0.2 ºC and a contact time of 45 min with constant stirring at 100 rpm. The highest removal rate was 99.94%, showing a positive correlation with adsorbent dose and temperature under acidic conditions and an inverse relationship with stirring speed. These findings confirm that HSOC is a highly effective, economical and promising alternative adsorbent for RB5 dye removal.

CONFLICT OF INTEREST

The authors declare that there is no conflict of interests regarding the publication of this article.

DECLARATION OF AI-ASSISTED TECHNOLOGIES

During the preparation of this manuscript, the authors used an AI-assisted tool(s) to improve the language. The authors reviewed and edited the content and take full responsibility for the published work.

REFERENCES

1. A.G. Meskel, M.M. Kwikima, B.T. Meshesha, N.G. Habtu, S.V.C.S. Naik and B.P. Vellanki, *Environ. Challenges*, **14**, 100829 (2024); https://doi.org/10.1016/j.envc.2023.100829
2. M. Cetina, P. Mihovilović, A. Pešić and B. Vojnović, *Molecules*, **30**, 2593 (2025); https://doi.org/10.3390/molecules30122593
3. A.M. Alotaibi, A.A. Aljabbab, M.S. Alajmi, A.N. Qadrouh, M. Farahat, M.A. Abdel Khalek, H. Baioumy, R.Y. Alzahrani, T.H. Mana and R.S. Almutairi, *Sustainability*, **17**, 3320 (2025); https://doi.org/10.3390/su17083320
4. H.J. Kim, J.W. Han, J.H. Yu, B.M. Jun and K. Chon, *Desalination Water Treat.*, **321**, 100970 (2025); https://doi.org/10.1016/j.dwt.2024.100970
5. M.C. Kasemodel, L.G. de Aguiar, V.G.S. Rodrigues and É.L. Romão, *Colorants*, **4**, 21 (2025); https://doi.org/10.3390/colorants4020021
6. S. Rajoriya, V.K. Saharan, A.S. Pundir, M. Nigam and K. Roy, *Curr. Res. Green Sustain. Chem.*, **4**, 100180 (2021); https://doi.org/10.1016/j.crgsc.2021.100180
7. M. Hosseinzehi, M. Khatebasreh and A. Dalvand, *Int. J. Environ. Anal. Chem.*, **102**, 6970 (2022); https://doi.org/10.1080/03067319.2020.1819991
8. A.E. Abdelhamid, A.E. Elsayed, M. Naguib and E.A.B. Ali, *Fibers Polym.*, **24**, 2391 (2023); https://doi.org/10.1007/s12221-023-00247-z
9. U. Hübner, S. Spahr, H. Lutze, A. Wieland, S. Rüting, W. Gernjak and J. Wenk, *Heliyon*, **10**, e30402 (2024); https://doi.org/10.1016/j.heliyon.2024.e30402.
10. C. Zhang, R. Yuan, H. Chen, B. Zhou, Z. Cui and B. Zhu, *Molecules*, **29**, 4267 (2024); https://doi.org/10.3390/molecules29174267
11. M.M. Naim, N.F. Al-Harby, M. El Batouti and M.M. Elewa, *Molecules*, **27**, 1593 (2022); https://doi.org/10.3390/molecules27051593
12. H.B. Rahmoun, M. Boumediene, A.N. Ghenim, E.F. Da Silva and J. Labrincha, *Environments*, **12**, 201 (2025); https://doi.org/10.3390/environments12060201
13. B. Naraghi, M.M. Baneshi, R. Amiri, A. Dorost and H. Biglari, *Electron. Physician*, **10**, 7086 (2018); https://doi.org/10.19082/7086
14. B.M. Thamer, F.A. Al-aizari and H.S. Abdo, *Molecules*, **28**, 7712 (2023); https://doi.org/10.3390/molecules28237712
15. B. Kumar, K. Agrawal, and P. Verma, *J. Hazard. Toxic Radioact. Waste*, **25**, 1 (2021); https://doi.org/10.1061/(ASCE)HZ.2153-5515.0000590
16. V. Ganthavee and A.P. Trzcinski, *Int. J. Environ. Sci. Technol.*, **22**, 1083 (2025); https://doi.org/10.1007/s13762-024-05696-4
17. M.X. Zhu, L. Lee, H.H. Wang and Z. Wang, *J. Hazard. Mater.*, **149**, 735 (2007); https://doi.org/10.1016/j.jhazmat.2007.04.037
18. M. Mohammadi-Galangash, S.K. Mousavi and M. Shirzad-Siboni, *Sci. Rep.*, **15**, 14314 (2025); https://doi.org/10.1038/s41598-025-95091-x
19. N.T. Nghia and V.D. Nguyen, *Molecules*, **30**, 2627 (2025); https://doi.org/10.3390/molecules30122627
20. A. Khasri, M.R.M. Jamir, A.A. Ahmad and M.A. Ahmad, *Desalination Water Treat.*, **216**, 401 (2021); https://doi.org/10.5004/dwt.2021.26852
21. T. Borklu Budak, *The European J. Res. Develop.*, **2**, 106 (2022); https://doi.org/10.56038/ejrnd.v2i4.168
22. P. De Luca and J. B. Nagy, *Materials*, **13**, 1 (2020); https://doi.org/10.3390/ma13235508
23. S. Dutta, B. Gupta, S.K. Srivastava and A.K. Gupta, *Mater. Adv.*, **2**, 4497 (2021); https://doi.org/10.1039/D1MA00354B
24. U.B. Deshannavar, P.G. Hegde, P.S. Patil, N. Tamburi, K. Ruchi, A. Kolur, A. Jadhav and M. El-Harbawi, *Desalination Water Treat.*, **210**, 415 (2021); https://doi.org/10.5004/dwt.2021.26543
25. G. Gentscheva, P. Vassileva, C. Tzvetkova, A. Pashev, I. Yotkovska, M. Mladenov and T. Vassilev, *Separations*, **12**, 258 (2025); https://doi.org/10.3390/separations12100258
26. N.T.H. Hoa, N.T. Quynh, V.D. Nguyen, T.N. Nguyen, B.Q. Huy, N.T. Thanh, H.T. Loan, N.T.Q. Hoa and N.T. Nghia, *Water*, **17**, 1678 (2025); https://doi.org/10.3390/w17111678
27. F.T. Zohra, S. Ahmed, M.Z. Alam, M. Nurnabi and N. Rahman, *Water Resour. Ind.*, **33**, 100281 (2025); https://doi.org/10.1016/j.wri.2025.100281
28. K. Phumivanichakit, T. Borsu, J. Maneerat, P. Kaewmaneerat and P. Wangsirikul, *Technol. Horiz.*, **42**, (2025); https://doi.org/10.55003/ETH.420308
29. P.L. Homagai, R. Poudel, S. Poudel and A. Bhattarai, *Heliyon*, **8**, e09261 (2022); https://doi.org/10.1016/j.heliyon.2022.e09261
30. S. Abbas, T. Javeed, S. Zafar, M.B. Taj, A.R. Ashraf and M.I. Din, *Desalination Water Treat.*, **233**, 387 (2021); https://doi.org/10.5004/dwt.2021.27538
31. E. Pagalan Jr., M. Sebron, S. Gomez, S.J. Salva, R. Ampusta, A.J. Macarayo, C. Joyno, A. Ido and R. Arazo, *Ind. Crops Prod.*, **145**, 111953 (2020); https://doi.org/10.1016/j.indcrop.2019.111953
32. F. Aouay, A. Attia, L. Dammak, R. Ben Amar and A. Deratani, *Materials*, **17**, 3078 (2024); https://doi.org/10.3390/ma17133078
33. T. Börklü Budak, *Molecules*, **28**, 6639 (2023); https://doi.org/10.3390/molecules28186639
34. A.M. Hardieka and T. Börklü Budak, *Molecules*, **30**, 3539 (2025); https://doi.org/10.3390/molecules30173539
35. A.H. Mangood, I. Abdelfattah, F.A. El-Saied and M.Z. Mansour, *Int. J. Environ. Anal. Chem.*, **103**, 4450 (2023); https://doi.org/10.1080/03067319.2021.1928102
36. B. Moralı and T. Börklü Budak, *Molecules*, **30**, 4039 (2025); https://doi.org/10.3390/molecules30204039
37. S. Farch, M.M. Yahoum, S. Toumi, H. Tahraoui, S. Lefnaoui, M. Kebir, M. Zamouche, A. Amrane, J. Zhang, A. Hadadi and L. Mouni, *Separations*, **10**, 60 (2023); https://doi.org/10.3390/separations10010060
38. M. Zhang, X. Liu, W. Li, Z. Tan, Q. Wang and L. Zhang, *Desalination Water Treat.*, **222**, 246 (2021); https://doi.org/10.5004/dwt.2021.27083
39. M. Pijović Radovanović, M. Ječmenica Dučić, D. Vasić Anićijević, V. Dodevski, S. Živković, V. Pavićević and B. Janković, *Processes*, **13**, 1715 (2025); https://doi.org/10.3390/pr13061715
40. M.I. Ismail, M.S.M. Fadzil, N.N.F. Rosmadi, N.R.A.M. Razali and A.R. Mohamad Daud, *J. Phys.: Conf. Ser.* **1349**, 012105, (2019); https://doi.org/10.1088/1742-6596/1349/1/012105
41. Z. Bencheqroun, I. El Mrabet, M. Nawdali, M. Benali and H. Zaitan, *Desalination Water Treat.*, **240**, 177 (2021); https://doi.org/10.5004/dwt.2021.27635
42. Y. Toptaş, B. Yavuz, A. Aksoğan Korkmaz and Y. Önal, *Int. J. Environ. Anal. Chem.*, **105**, 3372 (2025); https://doi.org/10.1080/03067319.2024.2346192
43. N. Morin-Crini, J.N. Staelens, S. Loiacono, B. Martel, G. Chanet and G. Crini, *J. Appl. Polym. Sci.*, **137**, 48823 (2020); https://doi.org/10.1002/app.48823
44. Y. Akköz and R. Coşkun, *Int. J. Biol. Macromol.*, **252**, 126447 (2023); https://doi.org/10.1016/j.ijbiomac.2023.126447

45. N. Morin-Crini, S. Loiacono, V. Placet, G. Torri, C. Bradu, M. Kostić, C. Cosentino, G. Chanet, B. Martel, E. Lichtfouse and G. Crini, *Environ. Chem. Lett.*, **17**, 393 (2019); https://doi.org/10.1007/s10311-018-0812-x
46. L.C. Cavalcante, K.Q. de Carvalho, F.J. Bassetti and L.A.A. Coral, *Desalination Water Treat*., **320**, 100606 (2024); https://doi.org/10.1016/j.dwt.2024.100606
47. I. Aminu, S.M. Gumel, W.A. Ahmad and A.A. Idris, *Am. J. Anal. Chem.*, **11**, 47 (2020); https://doi.org/10.4236/ajac.2020.111004
48. A. El Shahawy and G. Heikal, *RSC Adv.*, **8**, 40511 (2018); https://doi.org/10.1039/C8RA07221C
49. N.T.H. Hoa, N.T. Quynh, V.D. Nguyen, T.N. Nguyen, B.Q. Huy, N.T. Thanh, H.T. Loan, N.T.Q. Hoa and N.T. Nghia, *Water*, **17**, 1678 (2025); https://doi.org/10.3390/w17111678
50. A.B. Alemayehu and E. Alemayehu, "Optimization of Reactive Black 5 Dye Removal onto Kaolin Filter Cake Activated Carbon using Response Surface Methodology, *Research Square*, 3, (2024); https://doi.org/10.21203/rs.3.rs-5651884/v1
51. E. Kalkan, H. Nadaroğlu, N. Celebi and G. Tozsin, *Desalination Water Treat.*, **52**, 6122 (2014); https://doi.org/10.1080/19443994.2013.811114
52. N. Mengelizadeh and H. Pourzamani, *Health Scope*, **9**, e102443 (2020); https://doi.org/10.5812/jhealthscope.102443